Supplementary information for

Identifying efficient two-dimensional transition metal oxide cathodes for non-aqueous lithium-oxygen batteries using work function as a simple descriptor

Silan Chen[1], Lujie Jin[1], Yujin Ji[1]*, Youyong Li[1,2]*

[1]Institute of Functional Nano & Soft Materials (FUNSOM), Jiangsu Key Laboratory for Carbon-Based Functional Materials & Devices, Soochow University, Suzhou, Jiangsu 215123, China

[2]Macao Institute of Materials Science and Engineering, Macau University of Science and Technology, Taipa, Macau SAR 999078, China

*Corresponding author

Email address: yjji@suda.edu.cn (Y. Ji); yyli@suda.edu.cn (Y. Li);

Note S1

To systematically explore conductive two-dimensional transition metal oxides (2D TMOs), we extend our study to 356 unary 2D TMOs obtained from the Computational 2D Materials Database (C2DB). The screening protocol, summarized in **Fig. 4(a)**, involves filters for stability and electronic properties. First, high-level thermodynamic stability criteria are applied: (1) the heat of formation (ΔH) less than 0.20 eV/atom to ensure synthetic feasibility, (2) the convex hull energy (ΔH_{hull}) below 0.20 eV/atom to exclude metastable phases. Additionally, dynamic stability stiffness is enforced by requiring the non-negative minimum eigenvalue of the stiffness tensor (min{eig(C)}) to guarantee resistance to elastic deformation. These conditions identify 42 thermodynamically and mechanically stable candidates. Next, a zero bandgap (E_{gap}) constraint is imposed to select materials with intrinsic metallic behavior, as vanishing bandgaps are indicative of conductive electronic structures. This step refines the selection to 17 2D TMOs exhibiting both excellent stability and potential for high conductivity. This hierarchical approach establishes a rigorous foundation for further exploration of catalytic properties.

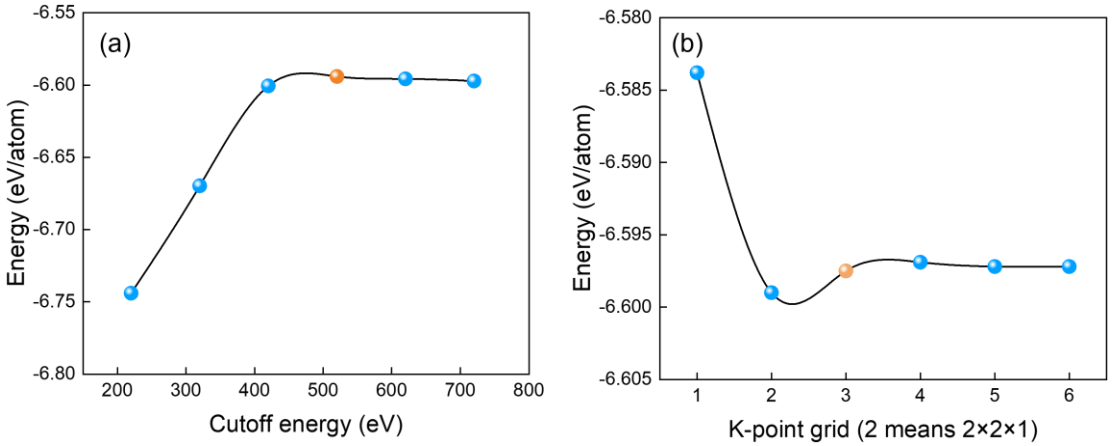

Fig. S1. Convergence tests for (a) cutoff energy and (b) k-point grid (exemplified with CoO_2).

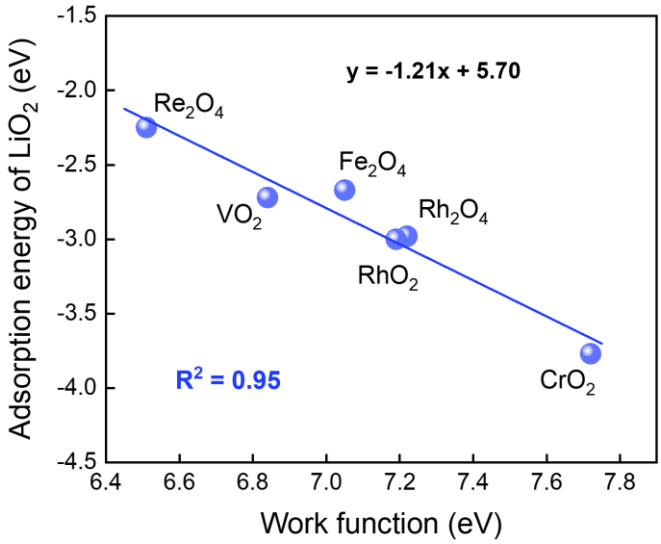

Fig. S2. Linear relationship between LiO_2 adsorption energy (E_{ads}) and work function (W_F) of pristine substrate material. (Based on DFT+U method.)

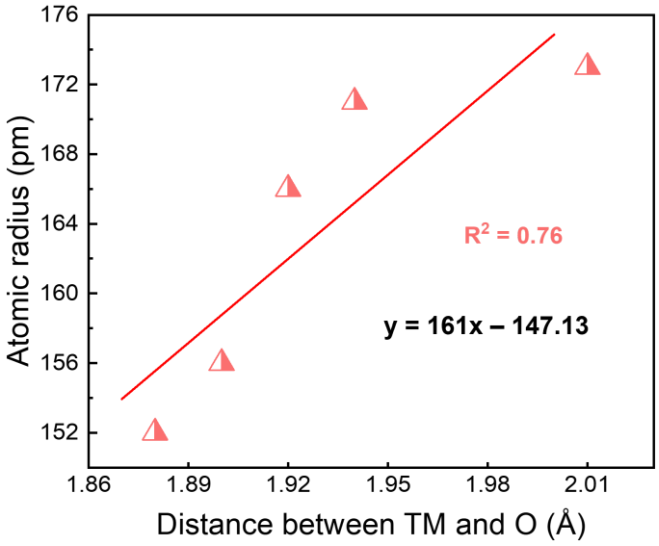

Fig. S3. The relationship between the TM-O bond length and TM atomic radius. The atomic radius used is calculated by Clementi et al.[1]

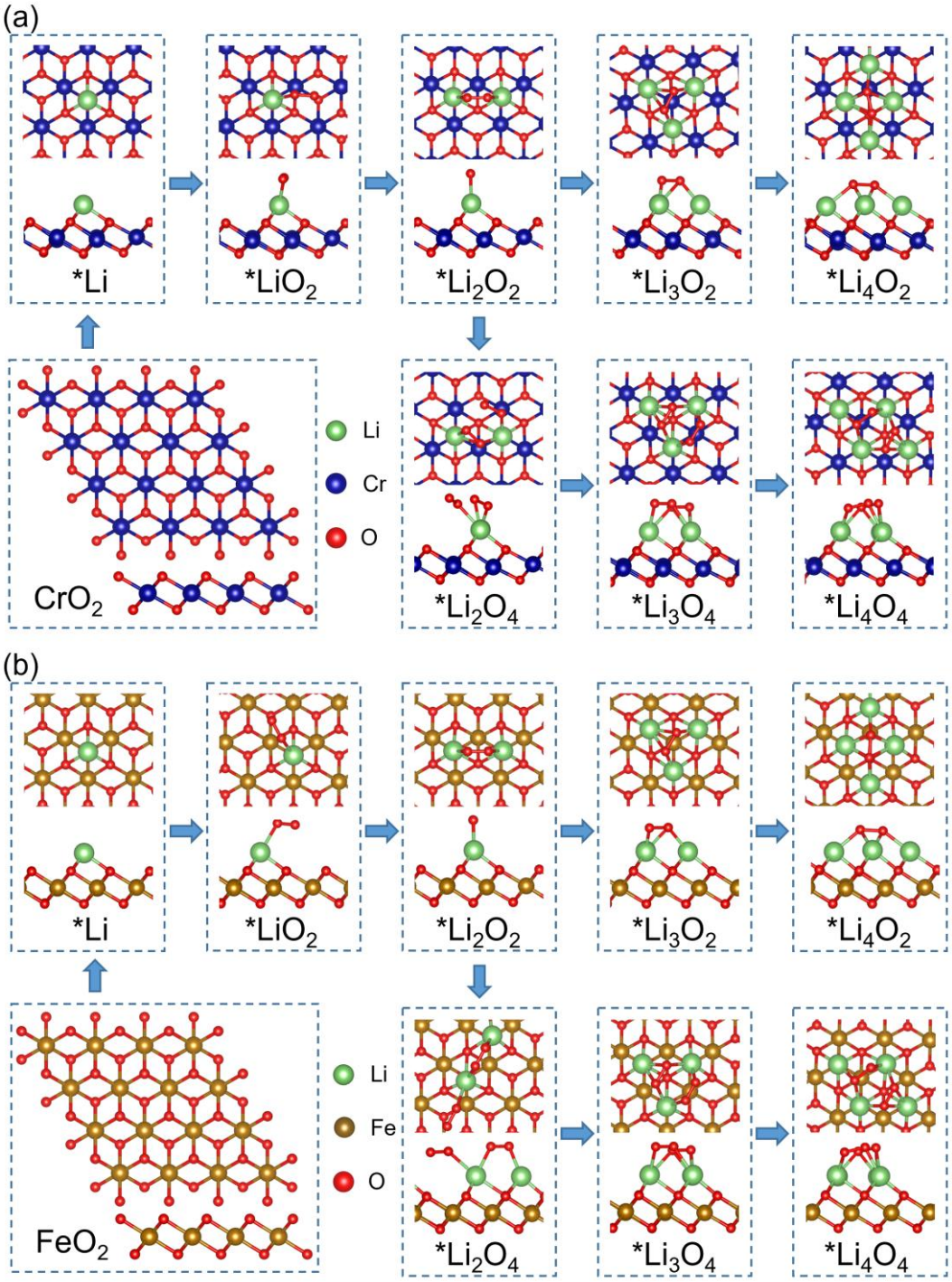
(a)
*Li
*LiO2
*Li2O2
*Li3O2
*Li4O2
CrO2
Li
Cr
O
*Li2O4
*Li3O4
*Li4O4
(b)
*Li
*LiO2
*Li2O2
*Li3O2
*Li4O2
FeO2
Li
Fe
O
*Li2O4
*Li3O4
*Li4O4

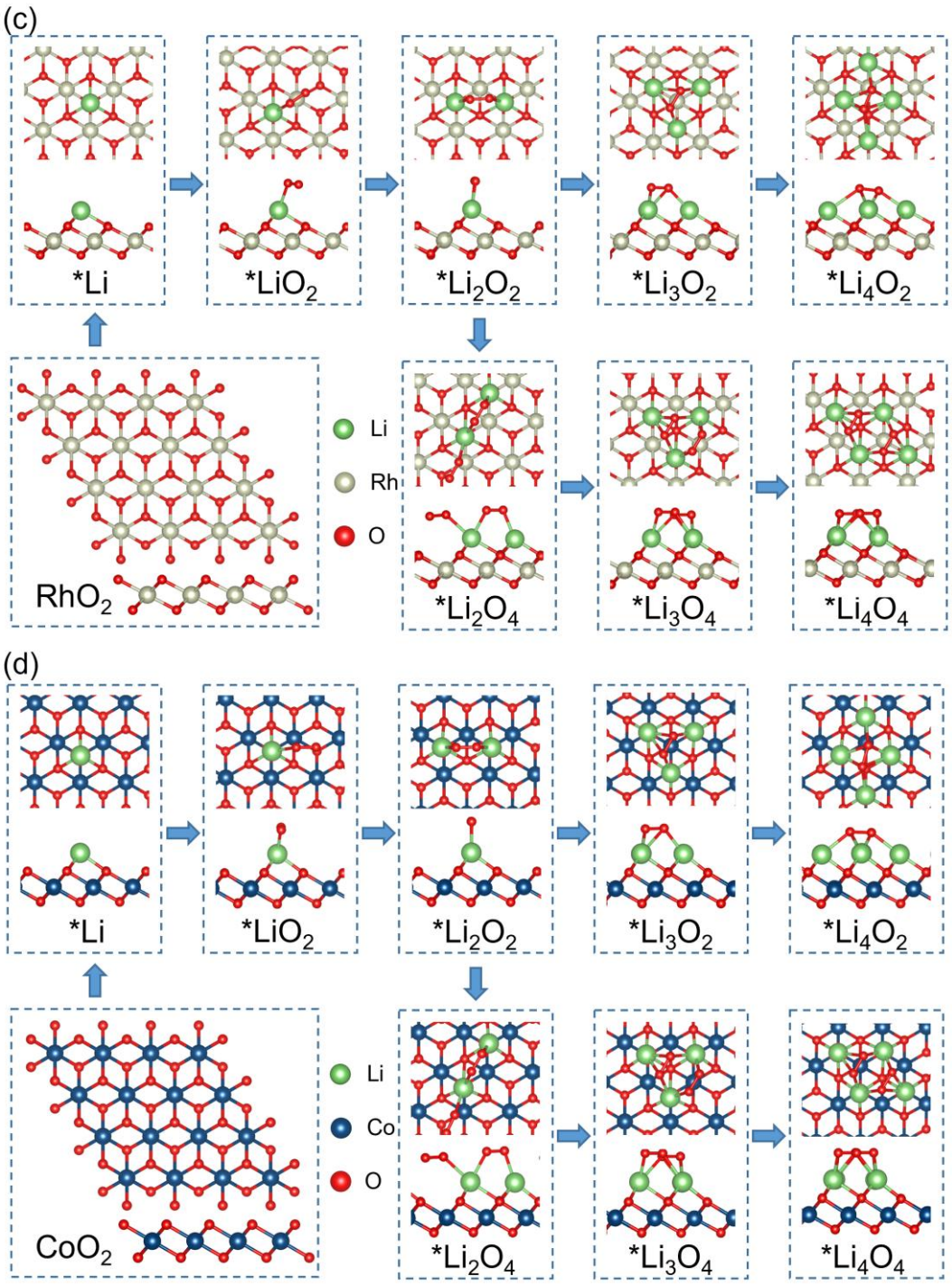

Fig. S4. The adsorption pathways and geometric configurations of the Li_xO_y species for the four-electron and two-electron reactions on the surfaces of (a) CrO_2, (b) FeO_2, (c) RhO_2 and (d) CoO_2.

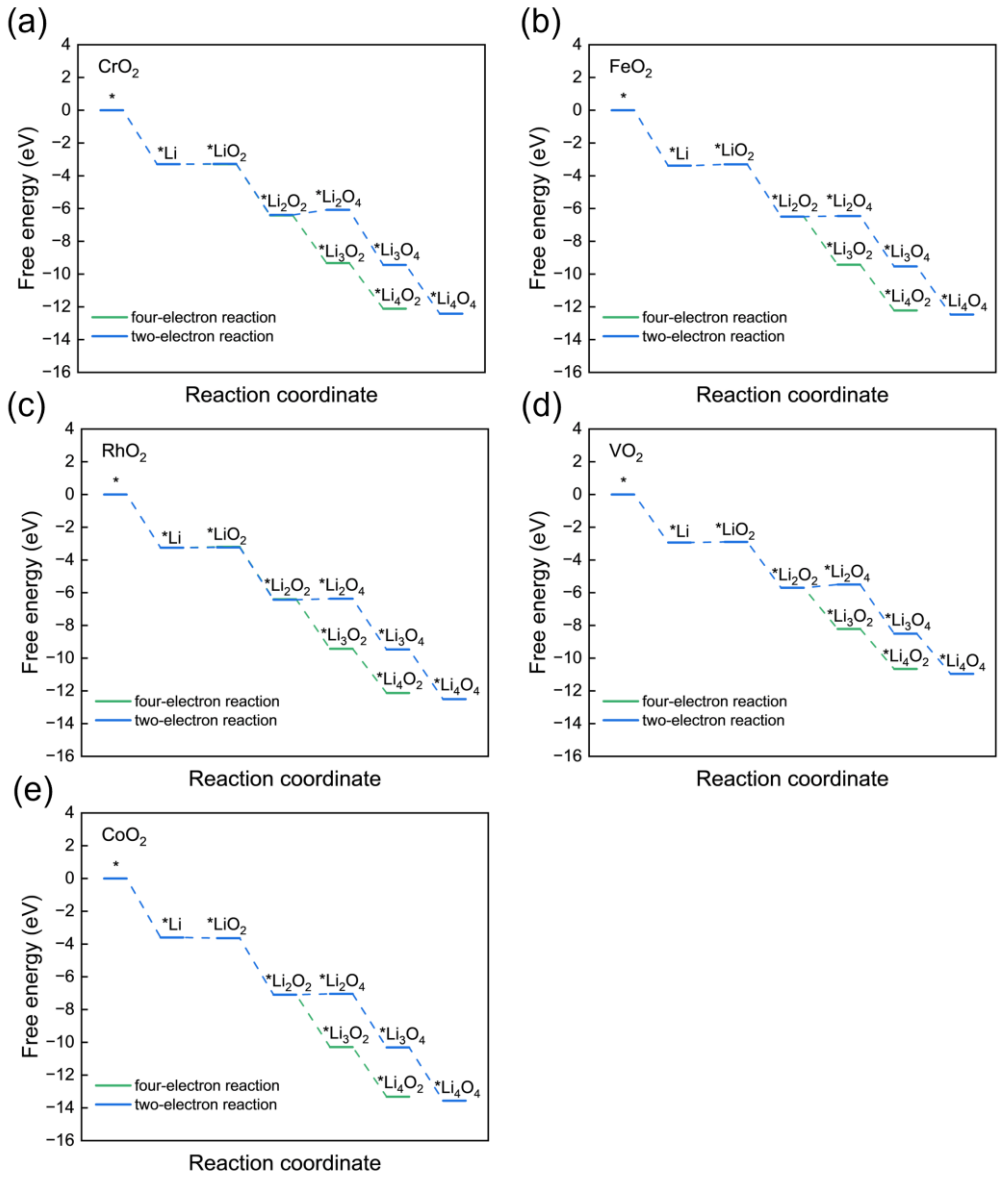

Fig. S5. The comparison of Gibbs energy profiles on the surfaces of (a) CrO_2, (b) FeO_2, (c) RhO_2, (d) VO_2 and (e) CoO_2 under different reaction pathways without any applied voltage.

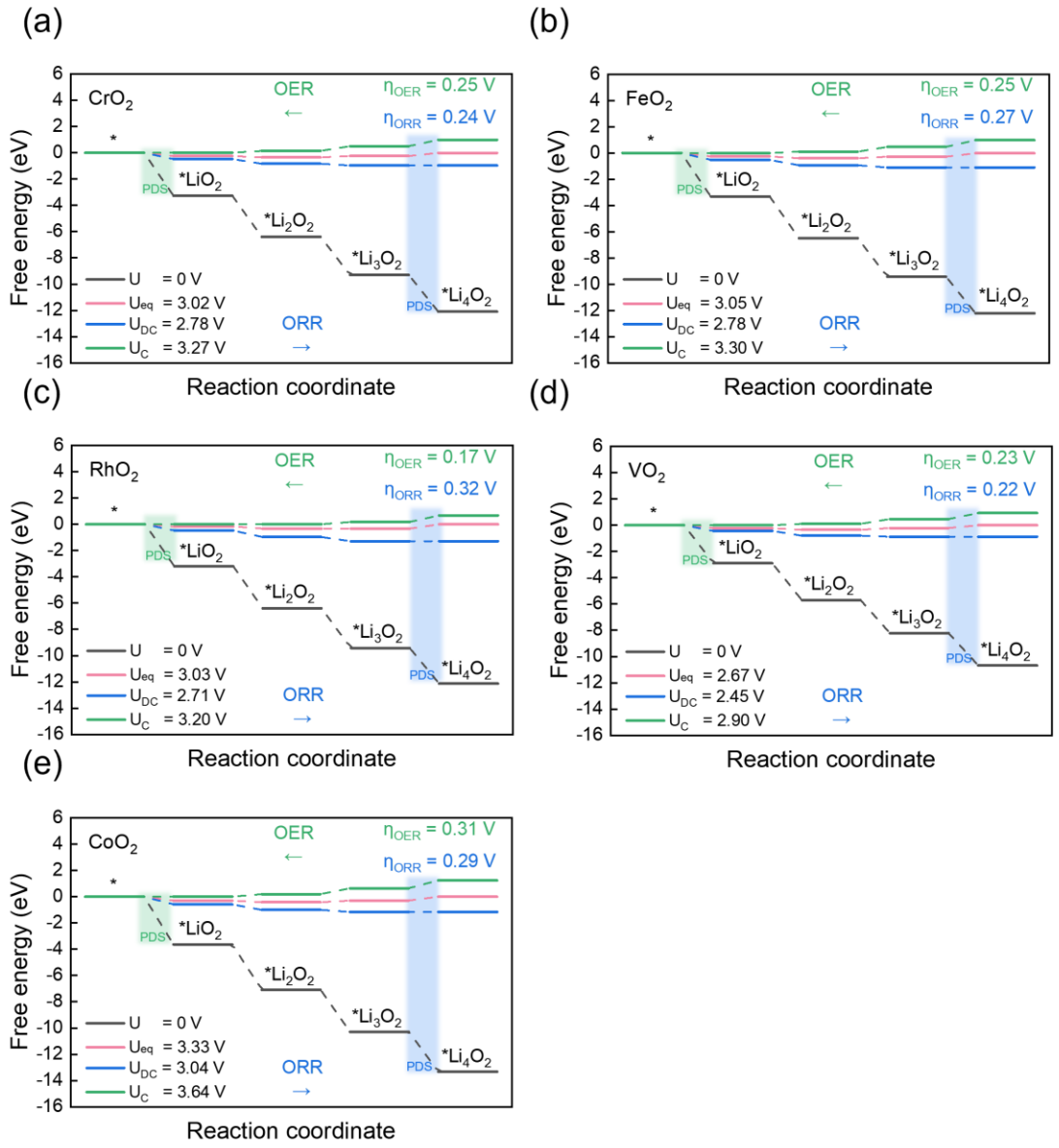

Fig. S6. Gibbs free energy diagrams following the four-electron reaction mechanism (*Li_4O_2 as the final product) on the surfaces of (a) CrO_2, (b) FeO_2, (c) RhO_2, (d) VO_2 and (e) CoO_2 under different applied voltages.

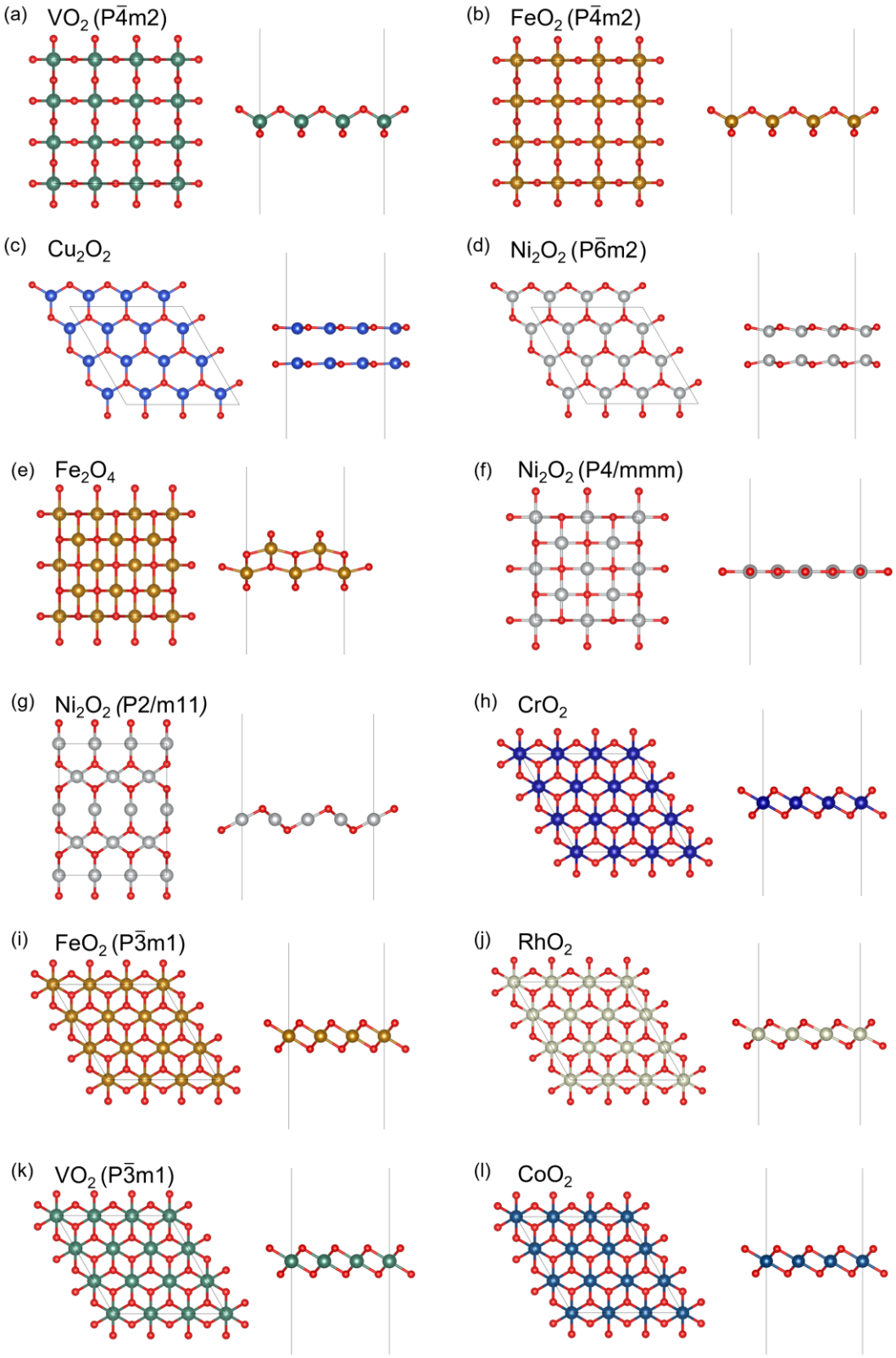
(a) VO_2 ($P\bar{4}m2$)
(b) FeO_2 ($P\bar{4}m2$)
(c) Cu_2O_2
(d) Ni_2O_2 ($P\bar{6}m2$)
(e) Fe_2O_4
(f) Ni_2O_2 (P4/mmm)
(g) Ni_2O_2 (P2/m11)
(h) CrO_2
(i) FeO_2 ($P\bar{3}m1$)
(j) RhO_2
(k) VO_2 ($P\bar{3}m1$)
(l) CoO_2

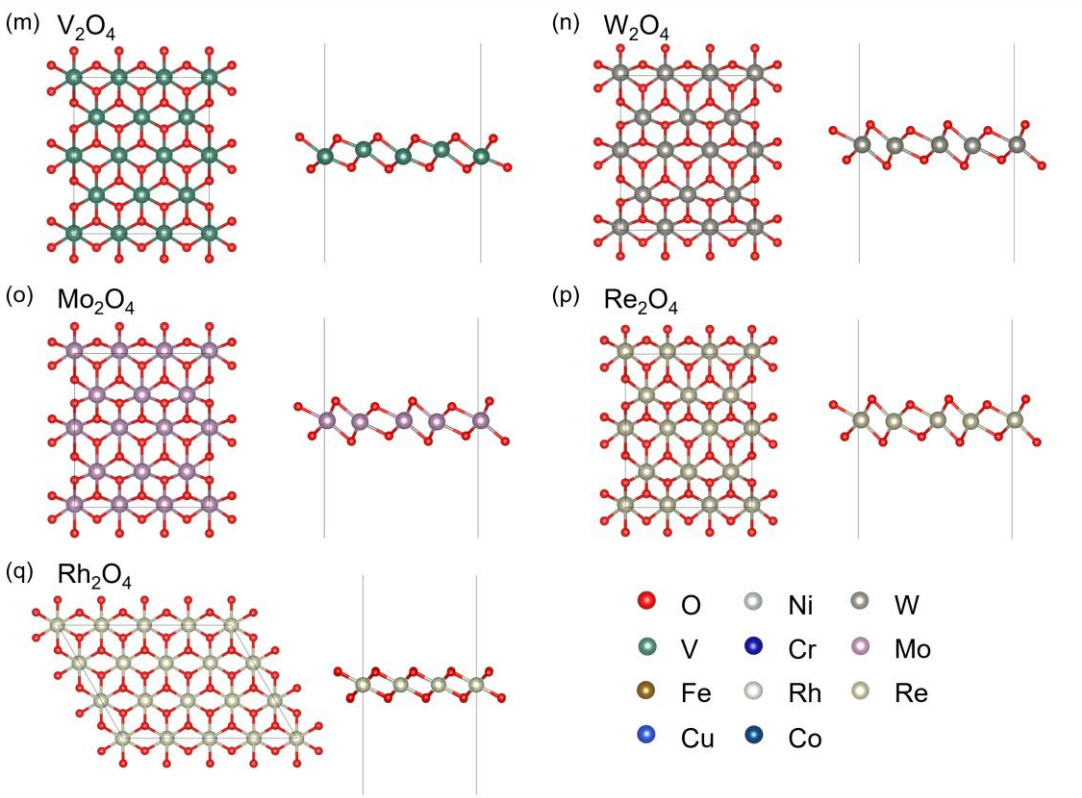

Fig. S7. Top view (left) and side view (right) of the optimized geometry of 17 kinds of 2D TMO materials.

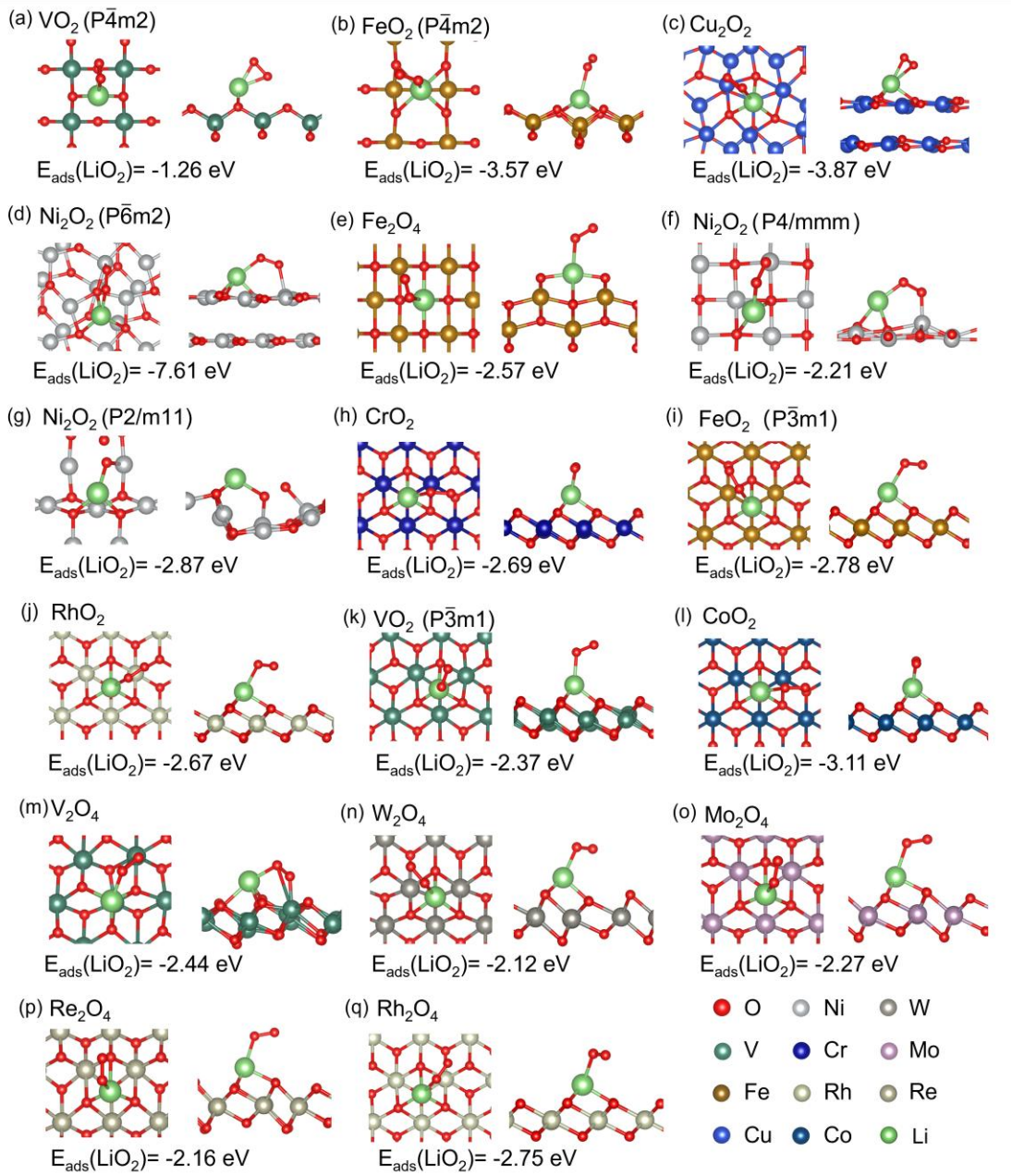

Fig. S8. The optimal configuration of 17 kinds of 2D TMO materials for adsorption of LiO_2. The top view is on the left and the side view is on the right.

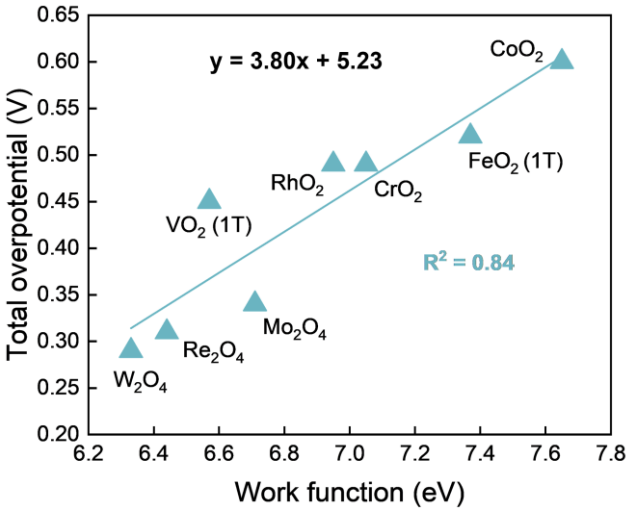

Fig. S9. Relationship between W_F and overall catalytic performance of 8 types of 2D TMOs materials.

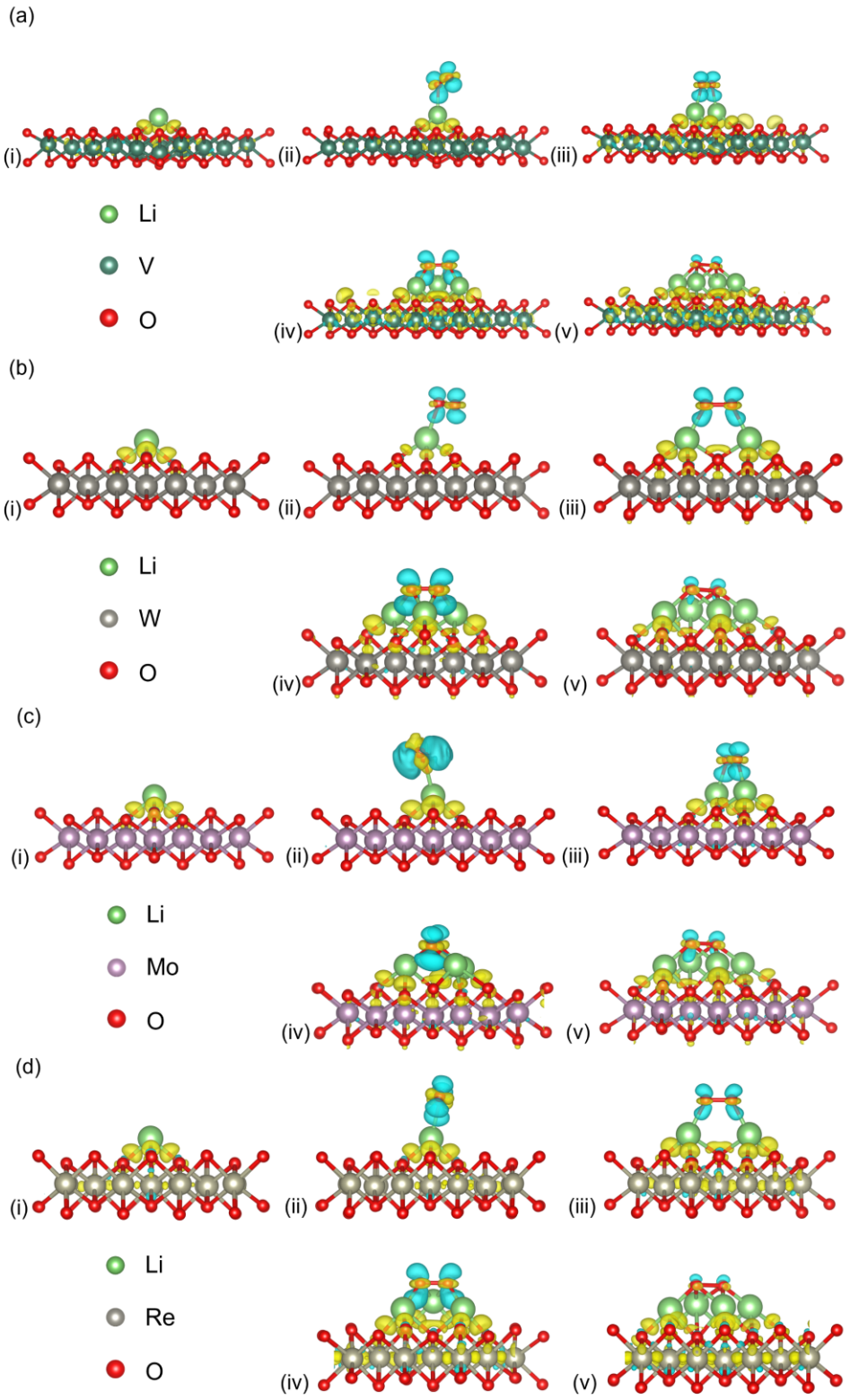

Fig. S10. Differential charge density plots of Li_xO_y on (a) VO_2, (b) W_2O_4, (c) Mo_2O_4, (d) Re_2O_4. Yellow indicates charge accumulation, while blue indicates charge depletion. Isosurface level = 0.006 a.u.

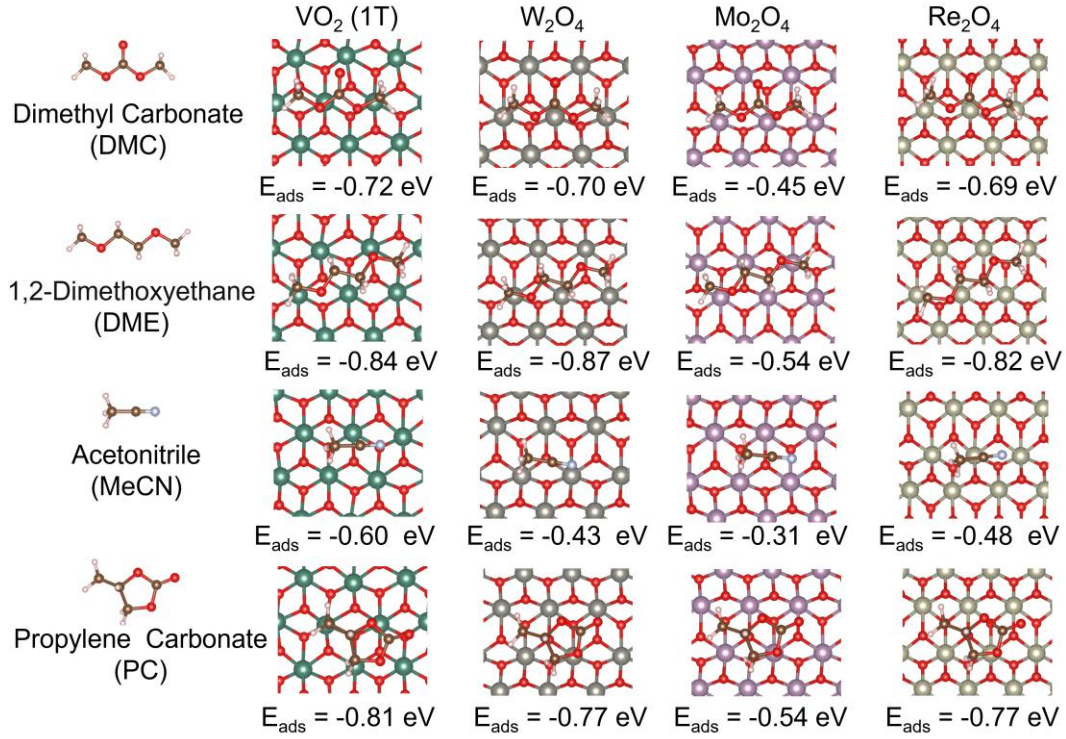

Fig. S11. The geometric adsorption configurations and adsorption energies of four common organic solvent molecules on the surfaces of VO_2, W_2O_4, Mo_2O_4, and Re_2O_4.

Table S1. The optimized lattice constant, the distance between atoms, and the bond angle. (The lattice constant and distance in Å, angle in °).

	a=b	d(TM-O)	θ(TM-O-TM)
CrO_2	2.89	1.92	97.5
FeO_2	2.80	1.90	95.1
RhO_2	3.08	2.01	100.3
VO_2	2.89	1.94	96.0
CoO_2	2.81	1.88	97.2

Table S2. The E_{ads} (eV) of intermediate product species Li_xO_y on the surfaces of 1T-TMOs (TM = Cr, Fe, Rh, V, Co).

Li_xO_y	CrO_2	FeO_2	RhO_2	VO_2	CoO_2
O_2	-0.17	-0.09	-0.11	-0.41	-0.14
Li	-3.31	-3.38	-3.26	-2.95	-3.71
LiO_2	-2.69	-2.78	-2.67	-2.37	-3.11
Li_2O_2	-4.42	-4.51	-4.42	-3.73	-5.11
Li_3O_2	-5.69	-5.75	-5.73	-4.62	-6.64
Li_4O_2	-7.21	-7.26	-7.19	-5.80	-8.44
Li_2O_4	-3.29	-3.43	-3.33	-2.71	-4.02
Li_3O_4	-4.90	-4.98	-4.87	-3.95	-5.78
Li_4O_4	-6.12	-6.15	-6.09	-4.53	-7.32

Table S3. Comparison of ORR and OER overpotential calculated theoretically for cathode catalysts.

Catalysts	η_{ORR} (V)	η_{OER} (V)	η_{TOT} (V)
CrO_2 (this work)	0.24	0.25	0.49
FeO_2 (this work)	0.27	0.25	0.52
RhO_2 (this work)	0.32	0.17	0.49
VO_2 (this work)	0.22	0.23	0.45
CoO_2 (this work)	0.29	0.31	0.60
W_2O_4 (this work)	0.16	0.13	0.29
Mo_2O_4 (this work)	0.16	0.18	0.34
Re_2O_4 (this work)	0.20	0.11	0.31
ZrO_2[2]	0.44	0.76	1.20
ZrS_2[2]	1.02	1.64	2.66
SL-SiC[3]	0.73	1.87	2.60
g-SiC_2[3]	0.85	2.20	3.05
g-SiC_2[3]	1.86	4.61	6.47
Phosphorene[4]	1.44	2.63	4.07
Graphene (Gr)[5]	0.57	0.29	0.86
N-Gr[5]	0.46	0.20	0.66
Gr/Cu[5]	0.11	0.26	0.37
N-Gr/Cu[5]	0.91	1.50	2.41
Cu[5]	1.91	1.90	3.81

Table S4. Space group, k-point grid set for majorization and E_{ads} (eV) of LiO_2 for 17 kinds of 2D TMOs.

Chemical formula	Space group	k-point grid	E_{ads} (LiO_2)	Chemical formula	Space group	k-point grid	E_{ads} (LiO_2)
VO_2	$P\bar{4}m2$	3×3×1	-1.26	RhO_2	$P\bar{3}m1$	3×3×1	-2.67
FeO_2	$P\bar{4}m2$	3×3×1	-3.57	VO_2	$P\bar{3}m1$	3×3×1	-2.37
Cu_2O_2	$P\bar{6}m2$	3×3×1	-3.87	CoO_2	$P\bar{3}m1$	3×3×1	-3.11
Ni_2O_2	$P\bar{6}m2$	3×3×1	-7.61	V_2O_4	$P2_1/m11$	3×2×1	-2.44
Fe_2O_4	Pmmn	3×3×1	-2.57	W_2O_4	$P2_1/m11$	3×2×1	-2.12
Ni_2O_2	P4/mmm	3×3×1	-2.21	Mo_2O_4	$P2_1/m11$	3×2×1	-2.27
Ni_2O_2	P2/m11	3×2×1	-2.87	Re_2O_4	$P2_1/m11$	3×2×1	-2.16
CrO_2	$P\bar{3}m1$	3×3×1	-2.69	Rh_2O_4	$P2_1/m11$	2×3×1	-2.75
FeO_2	$P\bar{3}m1$	3×3×1	-2.78				

References

1. E. Clementi, D. L. Raimondi and W. P. Reinhardt, *J. Chem. Phys.*, 1967, **47**, 1300-1307.
2. S. Lu, K. Zhu and X. Hu, *ACS Appl. Mater. Interfaces*, 2022, **14**, 13410-13418.
3. H. Dong, Y. Ji, T. Hou and Y. Li, *Carbon*, 2018, **126**, 580-587.
4. L. Kavalsky, S. Mukherjee and C. V. Singh, *ACS Appl. Mater. Interfaces*, 2019, **11**, 499-510.
5. J. Kang, J. S. Yu and B. Han, *J. Phys. Chem. Lett.*, 2016, **7**, 2803-2808.